Proceedings of the 12th International Conference on
Aluminium Alloys, September 5-9, 2010, Yokohama, Japan

pp. 1645-1649

Modeling for Anisotropic Foaming of Aluminum Precursor

Ryosuke Suzuki[1] and Koichi Kitazono[1]
[1]Graduate School of System Design, Tokyo Metropolitan University,
6-6 Asahigaoka, Hino, Tokyo, 191-0065, Japan.

Aluminum foams with unique cell structure are attractive for lightweight structural material. Precursor method is widely used for manufacturing the aluminum foam of near net-shape foaming. In the liquid state foaming, the expansion occurs isotropically. On the other hand, the expansion occurs anisotropically in the solid state. In the present study, the anisotropic foaming model was proposed for the anisotropic precursor. This model is based on creep expansion of the 2D-square cell by internal pressure and can calculate the time dependence of the foam shape change. In order to clarify the effectiveness of this model, the solid state foaming tests were carried out using the aluminum precursors manufactured by a powder metallurgical route. These precursors expanded parallel to the hot pressing direction preferentially. The 2D-square model agreed well with the experimental results.

Keywords: *Aluminum foam, Powder metallurgy, Anisotropy, Foaming behavior, Superplasticity.*

1. Introduction

Aluminum foams with cell structure are attractive for lightweight structural material for automotive, naval and other transport industrial applications [1]. For other industrial applications, aluminum foams are also attractive, because these have many excellent characteristics such as thermal absorption [2], sound absorption [3] and impact absorption [4]. The precursor method is widely used for manufacturing aluminum foams [5] because this method can make the products by near net-shape foaming.

In the case of a general precursor method, aluminum powder is first blended with an appropriate foaming agent and compacted by conventional powder metallurgical technique to produce a dense precursor. An aluminum foam is obtained by heating the precursor over the decomposition temperature of the foaming agent. In the liquid state, the expansion of the precursor occurs isotropically. On the other hand, the expansion occurs anisotropically in the solid state. This is because the texture is formed in the precursor during the hot compressing, extrusion and rolling processes. In order to clarify the foaming behavior of the precursor, a 3D-spherical model based on the creep expansion of the spherical vessel had been proposed by Dunand et al [6]. However, this model cannot calculate the anisotropic expansion. For near net-shape foaming, anisotropic foaming behavior should be clarified. In the present study, we propose a new 2D-square model in order to clarify the anisotropic foaming behavior.

2. Model Analysis

2.1 2D-square model

A 2D-square model is shown in Fig. 1. It is assumed that the foam consists of regularly-arranged square cells (Fig. 1(a)). Cell wall consists of elements i and ii which deform by internal pore pressure. The elements are assumed to deform according to the following creep constitutive equation:

$$\dot{\varepsilon} = K\sigma^n , \tag{1}$$

where $\dot{\varepsilon}$ is the strain rate, σ is the applied stress, K is the creep coefficient and n is the stress exponent. The strain rates of the x-direction for the element i and of the y-direction for element ii are expressed as

$$\dot{\varepsilon}_x^{\mathrm{i}} = \frac{\dot{l}_x}{l_x} = \frac{K}{\sqrt{2}}\alpha\left(\frac{1}{\sqrt{2}}P_{\mathrm{I}}\right)^n, \tag{2}$$

$$\dot{\varepsilon}_y^{\mathrm{i}} = \frac{\dot{l}_y}{l_y} = \frac{K}{\sqrt{2}}\alpha\left(\frac{1}{\sqrt{2}}P_{\mathrm{I}}\right)^n, \tag{3}$$

where P_{I} is the internal pore pressure and α is the anisotropic parameter($0 \le \alpha \le 1$). l_x is the size of x-direction for element i and l_y is the size of y-direction for the element ii. We assume that the internal pore pressure decreases with increasing the porosity according to Boyle's law. Then, P_{I} is expressed as

$$P_{\mathrm{I}} = \frac{f_0(1-f)}{f(1-f_0)}P_0, \tag{4}$$

where f_0 is the initial porosity and P_0 is the initial internal pore pressure. Thus, the strain rates of the x-direction for the element i and of the y-direction for the element ii can be calculated using Eqs. (1)-(4) as a function of porosity.

The porosity is expressed as

$$f = \frac{l_x l_y}{L_x L_y}, \tag{5}$$

where L_x and L_y are the sizes of x and y directions of the cell, respectively. From Eq. (5), the foaming rate, $\dot{f}$, is expressed as

$$\dot{f} = \frac{L_x L_y\left(\dot{l}_x l_y + l_x \dot{l}_y\right) - l_x l_y\left(\dot{L}_x L_y + L_x \dot{L}_y\right)}{\left(L_x L_y\right)^2}. \tag{6}$$

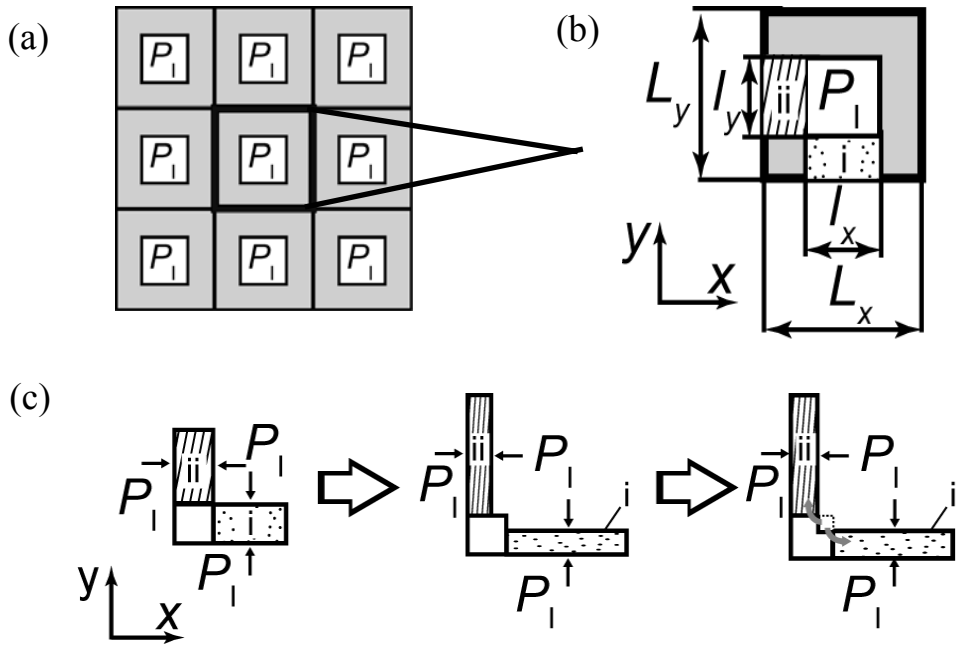

Fig. 1 Schematic illustration of the 2D-square model for solid-state foaming. The infinite body placed the square pores systematically (a), (b) the unit-square cell on the infinite body and (c) the deformation process of the elements i and ii in (b).

Since the volume of the cell walls keeps constant, the following equation is obtained.

$$\left(\dot{l}_x l_y + l_x \dot{l}_y\right) = \left(\dot{L}_x L_y + L_x \dot{L}_y\right). \tag{7}$$

By introducing Eq. (7) to Eq. (6), the foaming rate becomes

$$\dot{f} = f(1-f)\left(\frac{\dot{l}_x}{l_x} + \frac{\dot{l}_y}{l_y}\right). \tag{8}$$

By introducing Eqs. (2) and (3) to Eq. (8), the foaming rate becomes

$$\dot{f} = (1+\alpha)(1-f) f \frac{K}{\sqrt{2}}\left(\frac{P_\mathrm{I}}{\sqrt{2}}\right)^n. \tag{9}$$

By solving the differential equation (Eq. (9)), the porosity is obtained. In the case of n=1, above equation can be solved analytically.

$$f = \frac{2f_0 + (1+\alpha) f_0 K P_0 t}{2 + (1+\alpha) f_0 K P_0 t}. \tag{10}$$

On the other hand, we consider the change of the cell shape as L_x and L_y by introducing Eqs. (2) and (3) to Eq. (7). Eq. (7) becomes

$$\frac{\dot{L}_x}{L_x} - \frac{\dot{L}_y}{L_y} = f\left(\dot{\varepsilon}_x^{\mathrm{i}} - \dot{\varepsilon}_y^{\mathrm{ii}}\right). \tag{11}$$

Then, L_x and L_y are expressed as

$$\frac{\dot{L}_x}{L_x} = \alpha \frac{K}{\sqrt{2}} f\left(\frac{P_\mathrm{I}}{\sqrt{2}}\right)^n, \tag{12}$$

$$\frac{\dot{L}_y}{L_y} = \frac{K}{\sqrt{2}} f\left(\frac{P_\mathrm{I}}{\sqrt{2}}\right)^n. \tag{13}$$

In the case of n=1, L_y/L_x is expressed as

$$\frac{L_y}{L_x} = \left\{\frac{2 + (1+\alpha) K P_0 t}{2}\right\}^{\frac{1-\alpha}{1+\alpha}}. \tag{14}$$

2.2 Comparison between 2D-square and 3D-spherical models

The 2D-square model is compared with the 3D-spherical model [6]. The foaming rate of 3D-spherical model is expressed as

$$\dot{f} = \frac{3}{2} K \frac{f(1-f)}{\left(1 - f^{\frac{1}{n}}\right)^n}\left\{\frac{3}{2n}\left(P_\mathrm{I} - P_\mathrm{E}\right)\right\}^n, \qquad (P_\mathrm{I} \geq P_\mathrm{E}) \tag{15}$$

where P_E is the external pressure, and generally constant at atmospheric pressure ($P_\mathrm{E} \approx 0.1$ MPa). In the 2D-square model, we assume that the foaming stops at P_I=P_E. For calculation, we uses K=3.3×10^{-4} and n=2, which are material parameters of the superplastic 5083 aluminum alloy [7] when the precursor is heated at 853 K. In addition, f_0 is 0.6 % which is the volume fraction of the 1 mass% TiH_2, and P_0 is 535 MPa which is the pressure when hydrogen is released from a spherical TiH_2 particle with 45 μm diameter.

Porosities from the 2D-square and the 3D-spherical models are plotted as a function of foaming time, t_F (Fig. 2). At the beginning of foaming, the porosity increases rapidly in both models. The porosity calculated from the 3D-spherical model is slightly larger than that of the 2D-square model. At the end of foaming, two models have identical porosities. Therefore, the 2D-suquare model can also describe the isotropic foaming.

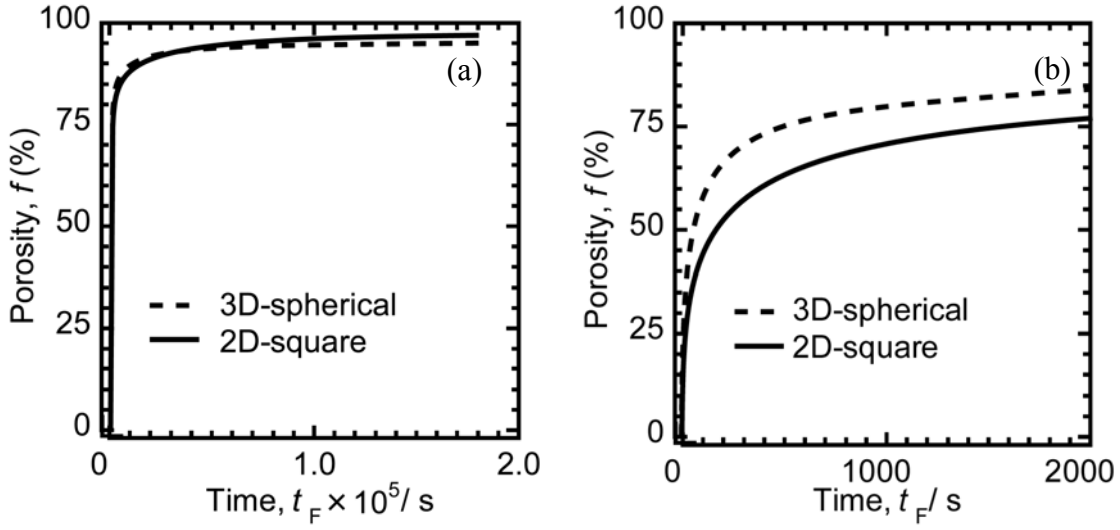

Fig. 2 Results of the calculations from the 3D-spherical and 2D-square models. (b) is a magnification of the early stage in (a).

3. Experimental Verification

3.1 Experimental procedure

Aluminum alloy powder less than 300 μm in size was obtained by machining a superplastic 5083 aluminum alloy plate [7]. TiH_2 powder less than 45 μm in size was used as a foaming agent. Aluminum alloy powder was mixed with 1 mass% TiH_2 powder. Cubic precursor with 30 mm diameter and 10 mm height was manufactured by uniaxial hot pressing at 753 K and 50 MPa for 60 min [8]. The relative density measured by Archimedes' method was more than 99 %. TiH_2 particles were homogeneously dispersed in the aluminum alloy matrix. Here, parallel and perpendicular to hot pressing directions are equal to y and x axes, respectively. Cubic specimen was inserted into an electric furnace and held at 873 K. The specimen temperature was measured by a thermocouple attached to a reference block. Size changes of the specimen before and after foaming were measured by a caliper.

3.2 Comparison between 2D-square model and experimental results

The experimental porosities are plotted as a function of foaming time (Fig. 3(a)). The experimental porosity increased with increasing the foaming time. The results of the calculation using 2D-square model are also plotted in Fig. 3(a). Here, we assume that the initial pore pressure is 66.3 MPa which is equal to the yield stress of the aluminum alloy. Anisotropic parameter is also unknown. We used α=0.5 in this study. The calculated porosity was lager than experimental porosity. In the case of the 2D-square model we did not consider the effects of the surface energy of pores and gas releasing. In the case of the experiment, insufficient superplastic deformation would occur because of the fine oxide dispersion during the powder metallurgy process.

The foam aspect ratio L_y/L_x is plotted as a function of foaming time (Fig. 3(b)). The experimental foam aspect ratio increased with increasing the foaming time. The calculated and experimental foam aspect ratio showed good agreement.

4. Conclusions

In order to calculate and discuss the expansion anisotropy, we proposed the 2D-square model which is based on creep deformation by internal pore pressure. In order to examine the adequacy and the

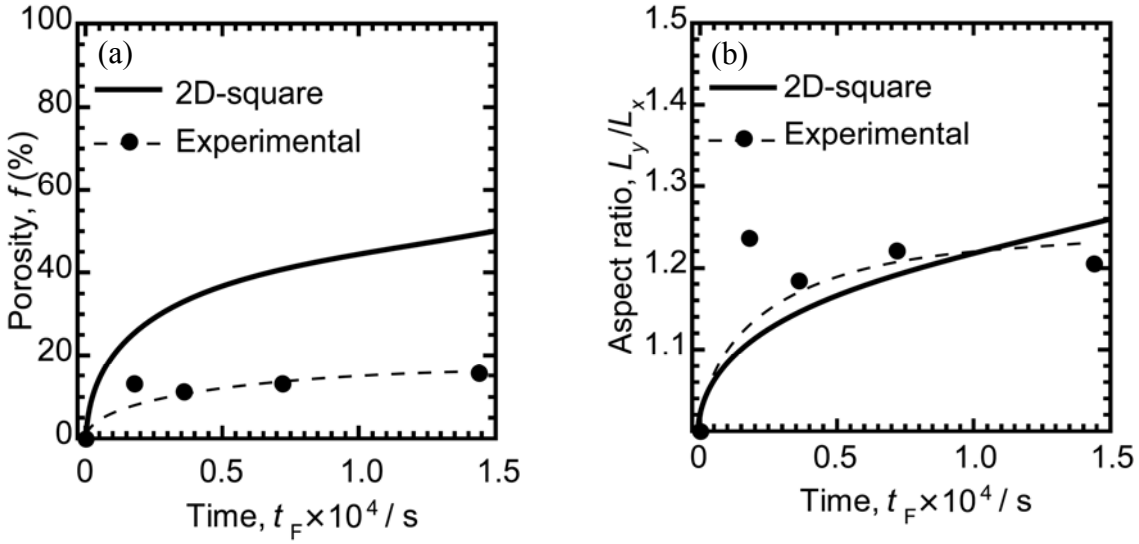

Fig. 3 Comparison of the model analysis with experimental results. The time dependency (a) of the porosity and (b) of the foam aspect ratio.

effectiveness of this model, 2D-square model is compared with the 3D-spherical model and investigated experimentally.

The porosity calculated from the 3D-spherical model is slightly larger than that of the 2D-square model. At the end of foaming, two models have identical porosities. Therefore, 2D-suquare model can describe the isotropic foaming.

The solid state foaming tests were carried out using the 5083 superplastic aluminum precursors manufactured by uniaxial hot pressing. These precursors expanded parallel to hot pressing direction preferentially. The experimental porosity increased with increasing the foaming time. The calculated porosity was lager than experimental porosity. In the case of the 2D-square model we did not consider the effects of the surface energy of pores and gas releasing. In the case of the experiment, insufficient superplastic deformation would occur because of the fine oxide dispersion during the powder metallurgy process. The calculated and experimental foam aspect ratio showed good agreement.

Acknowledgment

This study was supported in part by the Japan Aluminum Association.

References

[1] J. Baumeister, J. Banhart and M. Weber: Mater. Design 18 (1997) 217-220.
[2] K. Kitazono: Mater. Trans. 47 (2006) 2223-2228.
[3] T. L. Lu, A. Hess and M. F. Ashby: J. App. Phy. 85 (1999) 7528-7539.
[4] T. Mukai, H. Kanahashi, T. Miyoshi, M. Mabuchi T. G. Nieh and K. Higashi: Scripta Mater. 40 (1999) 921-927.
[5] N. Haydn and J. Wadley: Adv. Eng. Mater. 4 (2002) 726-733.
[6] N. G. D. Murray and D. C. Dunand: Acta Mater. 52 (2004) 2279-2291.
[7] H. Iwasaki, H. Hosokawa, T. Mori and T. Tagata: Mater. Sci. Eng. A252 (1998) 199-202.
[8] R. Suzuki and K. Kitazono: Proc. 6th International Conference on Porous Metals and Metallic Foams. (2010).
[9] A. Kennedy: Scr. Mater. 47 (2002) 763-767.
[10] F. Baumgärtner, I. Duarte and J. Banhart: Adv. Eng. Mater. 2 (2000) 168-174.
[11] I. Duarte and J. Banhart: Acta Mater. 48 (2000) 2349-2362.